

On the Use of a Bubble Formation Model to Calculate Diving Tables

D. E. YOUNT, Ph.D., and D. C. HOFFMAN, Ph.D.

*Department of Physics and Astronomy, University of Hawaii,
Honolulu, Hawaii 96822*

YOUNT DE, HOFFMAN DC. *On the use of a bubble formation model to calculate diving tables.* Aviat. Space Environ. Med. 1986; 57:149-56.

Previous decompression tables for humans were based upon unsupported assumptions because the underlying processes by which dissolved gas is liberated from blood and tissue were poorly understood. Some of those assumptions are now known to be wrong, and the recent formulation of a detailed mathematical model describing bubble nucleation has made it possible to calculate diving tables from established physical principles. To evaluate this approach, a comprehensive set of air diving tables has been developed and compared with those of the U.S. and British Navies. Conventional decompressions, altitude bends, no-stop thresholds, and saturation dives are all successfully described by one setting of four global nucleation parameters, which replace the U.S. Navy's matrices of M-values. Present air diving tables show great irregularity, even within sets created by the same authors. In contrast, this new approach is remarkably self-consistent, permitting accurate interpolation and extrapolation.

DECOMPRESSION sickness is caused by a reduction in ambient pressure, which results in supersaturation and the formation of gas bubbles in blood or tissue. This well-known disease syndrome, often called "the bends," is associated with such modern-day activities as deep-sea diving, working in pressurized tunnels and caissons, flying at high altitudes in unpressurized aircraft, and EVA excursions from spacecraft. A striking feature is that almost any body part, organ, or fluid can be affected including skin, muscle, brain and nervous tissue, the vitreous humor of the eye, tendon sheath, and bone. Medical

signs and symptoms range from itching and mild tingling sensations to crippling bone necrosis, permanent paralysis, and death.

The generality of the symptoms of decompression sickness and the fact that humans consist mainly of water suggest that the problem of bubble formation in the body may have a simple physical solution. Furthermore, since bubble formation occurs in almost any aqueous medium, the phenomenon can be studied in whatever substance is most convenient. A frequent choice in the series of experiments carried out at the University of Hawaii has been unflavored Knox gelatin, which is transparent and holds bubbles in place so that they can be counted and measured (12,13,23,24,25). Distilled water, sea water, agarose gelatin (3), and infertile hen's eggs (10) have also been used.

The main outcome of this line of investigation has been the development of the varying-permeability model (VPM), in which cavitation nuclei consist of spherical gas phases that are small enough to remain in solution and strong enough to resist collapse, their stability being provided by elastic skins or membranes consisting of surface-active molecules (18). Ordinarily, VPM skins are permeable to gas, but they can become effectively impermeable when subjected to large compressions, typically exceeding 8 atm.

By tracking the changes in nuclear radius that are caused by increases or decreases in ambient pressure, the varying-permeability model has provided precise quantitative descriptions of several of the bubble-counting experiments carried out in supersaturated gelatin (23,24,25). The model has also been used to trace levels of incidence for decompression sickness in a variety of animal species, including salmon, rats, and humans (15,16). Finally, microscopic

This manuscript was received for review in February 1985. The revised manuscript was accepted for publication in May 1985.

Address reprint requests to D.E. Yount, Ph.D., Dept. of Physics and Astronomy, University of Hawaii, Honolulu, HI 96822.

evidence has recently been obtained (19) which indicates that spherical gas nuclei—the persistent microbubbles hypothesized by the varying-permeability model—actually do exist and have physical properties consistent with those previously assigned to them (18,23–25). Nuclear radii, for example, are on the order of $1 \mu\text{m}$ or less, and the number density decreases exponentially with increasing radius (18,23–25). The exponential radial distribution is believed to be characteristic of a system of VPM nuclei in thermodynamic equilibrium, and it can be derived from statistical-mechanical considerations (17).

The most recent step in applying the varying-permeability model to decompression sickness has been to calculate a comprehensive set of air diving tables and to compare them with other tables now in use. Certain parts of this work have been reported already at scientific meetings (20,21), and a more detailed account is given here. The computational algorithms are described in the next section, and the results are discussed in the section which follows. A promising feature of the new tables is that they provide sensible prescriptions for a wide range of diving situations, yet they employ only four adjustable parameters and a single set of parameter values. All of the calculations reported here were initially carried out on a DEC VAX-11/780 and later duplicated on an ordinary home computer.

MATERIALS AND METHODS

Previous applications of the varying-permeability model to decompression sickness (15,16) involved rudimentary pressure schedules in which the subjects were first saturated with gas at some elevated pressure P_1 and then supersaturated by reducing the pressure from P_1 to the final setting P_2 . The data in such experiments are most easily presented by plotting the combinations of supersaturation versus exposure pressure ($P_{ss} \approx P_1 - P_2$ versus P_1) which yield a given morbidity, for example, a 50% probability of contracting decompression sickness. In order to describe these data, it was assumed that lines of constant morbidity were also lines of constant bubble number N (15,16). The bubble number, in turn, was assumed to be equal to the number of spherical gas nuclei with initial radii r_0 larger than some minimum radius r_0^{min} (18). This approach was remarkably successful, partly because the schedules involved were so simple—representing, as it were, a type of controlled experiment in which most of the variables in the problem were fixed.

The naive assumption of constant nucleation or constant bubble number does not encompass the full range of conditions covered by modern diving tables. That is, it yields a set of tables which, though they may be very safe, do not track conventional tables in their global behavior and often require total ascent times that would generally be considered excessive by the commercial diving industry. Given these circumstances, a decision was made to treat the conventional tables as valid experimental data and reformulate the decompression criterion accordingly.

The first step was to replace “constant bubble

number” with a “critical-volume hypothesis,” thereby assuming that signs or symptoms will appear whenever the total volume V accumulated in the gas phase exceeds some designated critical value V_{crit} . Although V_{crit} itself is fixed for all of the diving tables, gas is continuously entering and leaving the gas phase. In this sense, the new decompression criterion is dynamic, rather than static as in other applications of the critical-volume point of view (7).

The idea that gas is continuously leaving the gas phase is suggested by previous applications (15,16), which seem to imply that there is a bubble number N_{safe} which can be tolerated indefinitely, regardless of the degree of supersaturation P_{ss} . From this, it was deduced that the body must be able to dissipate free gas at a useful rate that is proportional both to N_{safe} and to P_{ss} . A possible rationale is provided by physiological studies which demonstrate that, so long as its capacity is not exceeded, the lung is able to continue functioning as a trap for venous bubbles (2).

Another implication of the present investigation is that in practical diving tables (and especially in surface-decompression procedures), the actual number of supercritical nuclei N_{actual} is allowed temporarily to exceed the number which can be tolerated indefinitely N_{safe} . This permits the volume of the gas phase to inflate at a rate that is proportional to $P_{ss}(N_{\text{actual}} - N_{\text{safe}})$. In the present formulation, the increase in gas-phase volume continues until P_{ss} is zero. At this point, usually long after the dive has ended, the net volume of released gas has reached its maximum value V_{max} , which must be less than V_{crit} if signs and symptoms of decompression sickness are to be avoided.

Computation of a diving table begins with the specification of six nucleation parameters. These are the surface tension γ , the nuclear skin compression γ_c (18), the minimum initial radius r_0^{min} (18), the time constant τ_R for the regeneration of nuclei crushed in the initial compression (17), and a composite parameter λ which is related to V_{crit} and determines, in effect, the amount by which bubble number N_{actual} can exceed the safe bubble number N_{safe} . N_{actual} is much larger than N_{safe} for short dives, but the two are nearly equal for dives of long duration.

From the given set of parameter values, the program calculates a preliminary estimate of P_{ss} that is just sufficient to probe the minimum initial radius r_0^{min} and hence to produce a number of bubbles equal to N_{safe} . In the permeable region of the model, which includes the great majority of air diving tables, the nuclear radius r_1^{min} following an increase in pressure from P_0 to P_1 can be obtained from the equation (18):

$$(1/r_1^{\text{min}}) = (1/r_0^{\text{min}}) + (P_1 - P_0)/2(\gamma_c - \gamma) \quad \text{Eq. 1}$$

Regeneration of the nuclear radius is allowed to take place throughout the time τ_R during which the pressure is held at P_1 . Regeneration may occur through a complex statistical-mechanical process (17), which is approximated here via an exponential decay with regeneration time constant τ_R :

$$r(t_R) = r_1^{\min} + (r_0^{\min} - r_1^{\min})[1 - \exp(-t_R/\tau_R)] \quad \text{Eq. 2}$$

The supersaturation P_{ss}^{\min} that is just sufficient to probe r_0^{\min} is then found from (18):

$$P_{ss}^{\min} = 2(\gamma/\gamma_c)(\gamma_c - \gamma)/r(t_R) \quad \text{Eq. 3}$$

Holding P_{ss}^{\min} fixed, the program next calculates a decompression profile and the total decompression time t_D . From t_D a new value of P_{ss}^{new} is obtained which will probe a new initial radius r_0^{new} that is smaller than r_0^{\min} and hence will result in a number of bubbles that is larger than N_{safe} . The relevant equation,

$$P_{ss}^{\text{new}} = [b + (b^2 - 4c)^{1/2}]/2 \quad \text{Eq. 4a}$$

where:

$$b = P_{ss}^{\min} + \lambda\gamma/[\gamma_c(t_D + H/0.693)] \quad \text{Eq. 4b}$$

$$c = (\gamma/\gamma_c)^2\lambda(P_1 - P_0)/(t_D + H/0.693) \quad \text{Eq. 4c}$$

is derived in the Appendix and must be evaluated for each tissue half-time H . Using the respective values of P_{ss}^{new} for each "tissue compartment," the program determines a more severe decompression profile, which will yield updated values of t_D and P_{ss}^{new} . After several iterations, t_D and P_{ss}^{new} converge, implying that V_{max} now differs from V_{crit} by an acceptably small amount.

The uptake and elimination of inert gas by the body are assumed to be exponential, as in conventional tables. Water vapor pressure and the dissolved partial pressures of oxygen and carbon dioxide are calculated in the manner described by Yount and Lally (22). The net contribution of these "active" gases is nearly constant at 102 mm Hg for inspired oxygen pressures up to about 2 ATA (22). This limit is not reached for air decompression tables at ambient pressures below about 10 ATA. The half-times H for the various "tissue compartments" are nominally 1, 2, 5, 10, 20, 40, 80, 120, 160, 240, 320, 400, 480, 560, and 720 min, but the 1-min tissue is never used. The onset of impermeability, $P^* = 9.2$ ATA, is high enough so that nearly all of the tables presented here lie in the "permeable" or "linear" region of the VP model, and hence this parameter can also be deleted (15,18).

Since the model predictions depend only upon the ratios γ/γ_c and $2\gamma/r_0^{\min}$, the setting of γ is essentially arbitrary (15,18). To be definite, however, a value of $\gamma = 17.9$ dyn/cm was selected (4). With this choice, the values of the remaining four parameters are $\gamma_c = 257$ dyn·cm⁻¹, $r_0^{\min} = 0.80\mu\text{m}$, $\tau_R = 20160$ min, and $\lambda = 7500$ fsw·min. These were found by requiring that the total decompression times in the new tables resemble those in the Tektite saturation dive (1) and in the U.S. Navy (USN) (14) and Royal Naval Physiological Laboratory (RNPL) (11) manuals. In other words, all of the results

reported in this paper were obtained by optimizing the values of only four adjustable parameters, γ_c , r_0^{\min} , τ_R , and λ , which replace the U.S. Navy's matrix of M-values (14).

The settings of the nucleation parameters listed in the previous paragraph differ somewhat from those given earlier (20,21). This is the result of three changes that have been made in the computer program. The first terminates the regeneration time t_R at the moment when decompression begins. The second corrects for the fact that tissue half-times H were being used in Eqs. 4a-c in place of exponential time constants $H/\ln(2) = H/0.693$. Finally, the exact quadratic solution given in Eqs. 4a-c has replaced the previous linear expression (20,21) obtained by setting c equal to zero. (See the Appendix for further details). With these compensating changes in the program and parameter values, the actual diving tables have remained essentially intact.

Depths and pressures are usually given in feet of sea water (33 fsw = 10 msw = 1 atm = 2 ATA, etc.) for convenience in making comparisons with the Tektite, USN, and RNPL reference schedules. For similar total decompression times, the set of tables generated in this study is expected to yield smaller total bubble volumes and therefore to be safer. However, none of the tables has yet been tested on either animal or human subjects.

RESULTS

In this section, the salient features of a number of diving tables using air as the breathing mixture are compared. The VPM and USN (14) profiles for an "exceptional exposure" involving greater than normal risk are shown in Fig. 1. In both cases, the descent and ascent rates are 60 fsw·min⁻¹, and the 3.33 min required to reach 200 fsw is counted as part of the 60-min "bottom time." The total decompression times are similar, the important difference being the deeper "first stop" of the VPM schedule, 130 fsw versus 60 fsw for USN. This is a persistent feature of the literally hundreds of comparisons that have been made of VPM tables with a variety of conventional tables now in use. The calculations indicate that the longer "first pull" of these conventional tables results in a larger supersaturation P_{ss} , in a larger bubble number N , and ultimately in a larger maximum volume of released gas V_{max} .

VPM, USN (14), and RNPL (11) "no-stop" decompressions are compared in Fig. 2, along with various "practical observations" compiled by Leitch and Barnard (9). Although there are some differences in this plot in the rates of descent and ascent and in the exposure conditions (9), the absence of prolonged decompression stages makes this type of "data" nearly independent of the overall surfacing strategy. The VPM curve follows very closely the RNPL points at depths up to 140 fsw and passes through the USN point at 5 min, 190 fsw. Over the entire range, it serves as a safe, tight, and therefore useful lower bound. The fact that the VPM curve is systematically lower than most of the "data" reflects the general conservatism of the tables as a whole. A bolder, more aggressive set of tables could, of course, be computed by simply adjusting the values of the nucleation parameters.

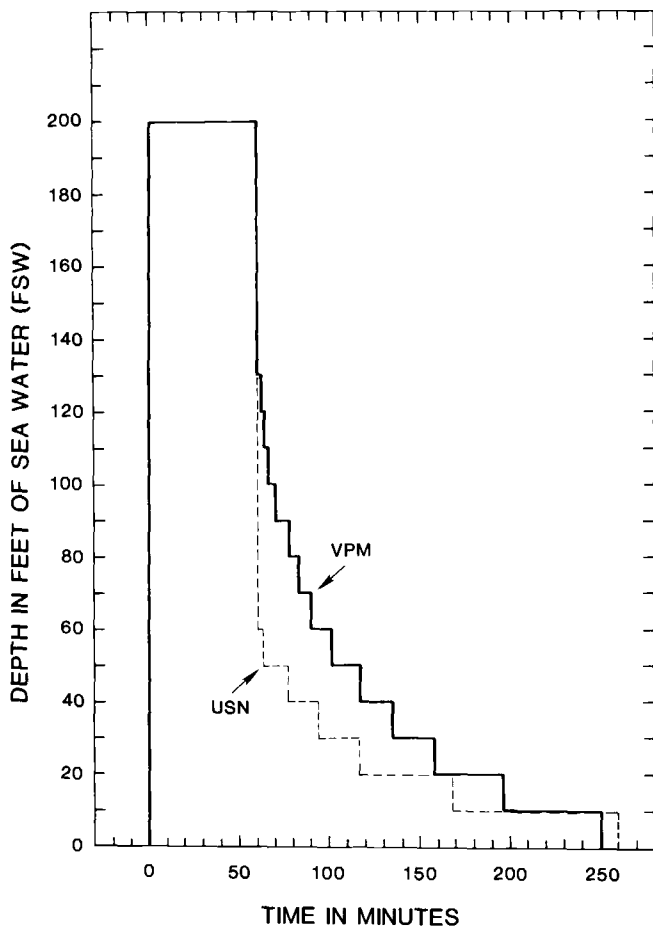


Fig. 1. Varying-permeability model (VPM) and U.S. Navy (USN) decompression profiles for a 60-min dive to 200 fsw. The longer "first pull" of conventional tables results in a larger supersaturation P_{ss} , a larger bubble number N , and ultimately in a larger maximum volume of released gas V_{max} .

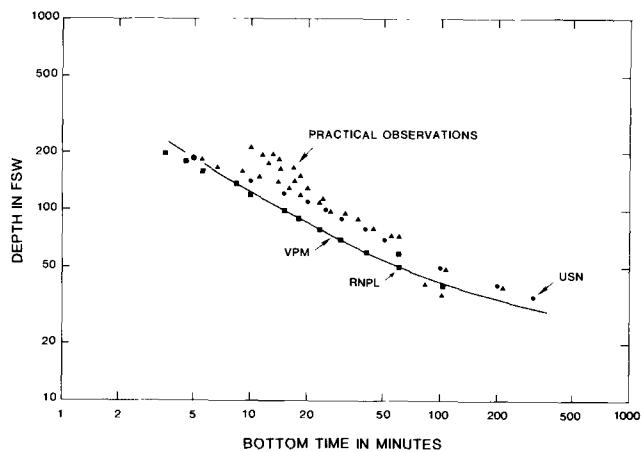


Fig. 2. Comparison of varying-permeability model (VPM), U.S. Navy (USN), and Royal Naval Physiological Laboratory (RNPL) "no-stop" decompressions with various practical observations, i.e., combinations of depth and bottom time which yielded no symptoms or only the mildest symptoms. The VPM curve follows very closely the RNPL points at depths up to 140 fsw and passes through the USN point at 5 min, 190 fsw. Over the entire range, it serves as a safe, tight and, therefore, useful lower bound.

Total ascent times for VPM, USN (14), and RNPL (11) are plotted as a function of the bottom time at 200 fsw in Fig. 3. The VPM curve lies close to the USN points for bottom times that extend all the way from 5 to 360 min. The large difference in USN and RNPL total ascent times (often more than a factor of 2) illustrates the wide divergence in opinion that still exists, even among highly-respected investigators in the diving field.

One very practical reason for attempting to optimize decompression procedures from first principles is the hope that if a correct global theory can someday be formulated, it will then be possible to relate and describe the whole range of decompression experience with a small number of equations and parameter values. Instead of "titrating" a handful of "volunteers" to develop a new table or determine a new "M-value" (14), a method which necessarily has limited statistical accuracy, one will be able to use an already-calibrated theory to interpolate or extrapolate, thereby bringing to bear the full statistical weight of a much larger data base. This idea is illustrated in Fig. 4, which connects the no-stop decompressions in Fig. 2 with the 14-d, 100-fsw Tektite saturation dive (1). The latter has been used by humans without incident. However, the close agreement apparent in this graph is partly fortuitous because the Tektite stops were 5 rather than 10 fsw

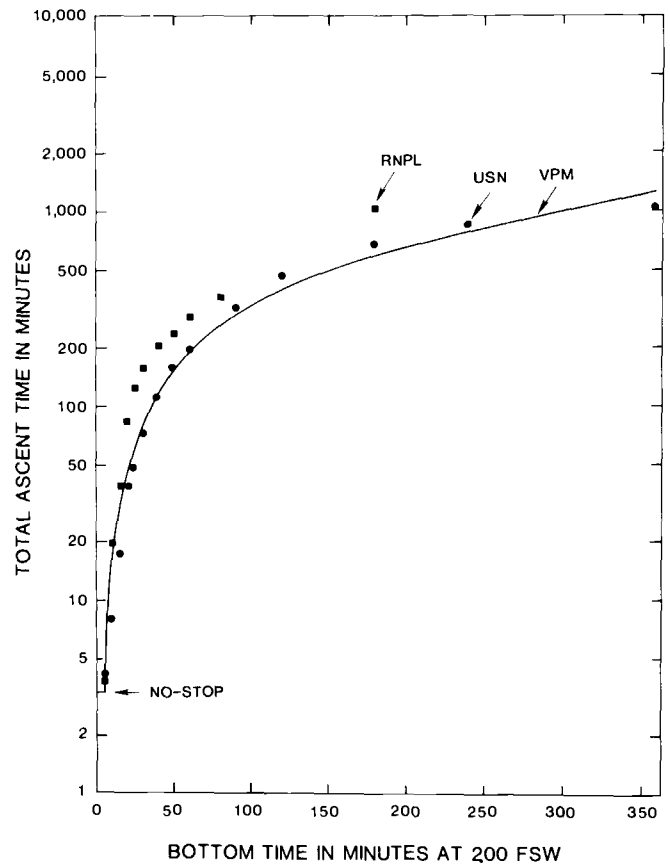


Fig. 3. Total ascent times versus bottom times at 200 fsw for VPM, USN, and RNPL decompression tables. The total ascent times for USN and RNPL often differ by more than a factor of 2.

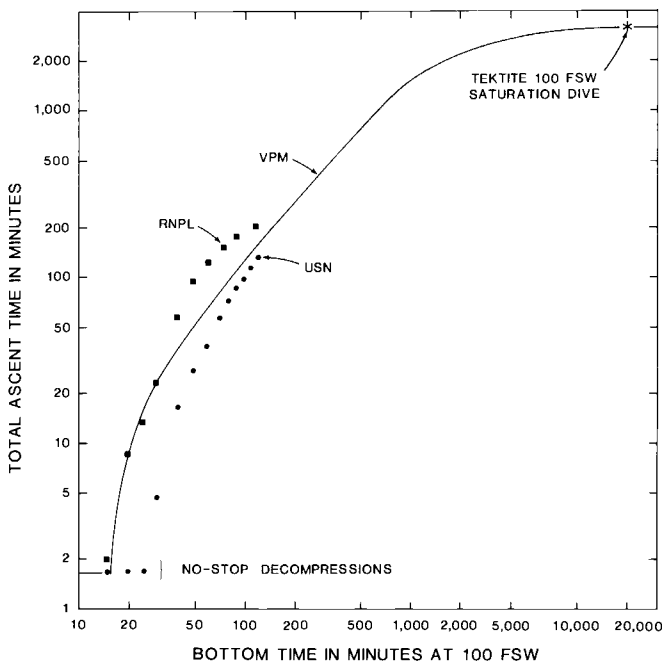


Fig. 4. Total ascent times versus bottom times at 100 fsw for VPM, USN, RNPL, and TEKTITE decompression tables. All of the VPM schedules reported in this paper were computed with the same values of the four adjusted nucleation parameters γ_c , r_0^{min} , τ_r , and λ .

apart, and the breathing gas was a normoxic oxygen-nitrogen mixture rather than air. In addition, both air and pure oxygen were breathed during various stages of the Tektite decompression. A more precise comparison is given in Table I, where the VPM schedule was calculated for a 14-d exposure to the 126 fsw equivalent air depth (22) of the Tektite dive.

By replacing the earlier assumption of constant bubble number with a dynamic critical-volume hypothesis, a comprehensive set of air diving tables has been prepared which, although untested, appears in all respects to be quite reasonable. It should not be forgotten, however, that the constant-bubble-number criterion did work well in those rudimentary cases in which it was first applied (15,16). This raises the question of whether the new and different criterion can also describe these special situations. The answer is affirmative, suggesting that the tables obey a kind of "correspondence principle" in which "critical volume" becomes equivalent to "constant bubble number" in the limit of a nucleation-dominated regime, i.e., a regime in which N_{actual} approaches N_{safe} and the allowed supersaturation P_{ss} is determined directly by r_0^{min} .

An illustration of the critical-volume ↔ critical-nucleation correspondence for humans is provided by Fig. 5. The rudimentary cases referred to in this figure, in the previous paragraph, and also at the beginning of the methods section are those in which the subjects are first saturated with gas at some elevated pressure P_1 and then supersaturated by reducing the pressure from P_1 to the final setting P_2 . In experiments with human subjects, $P_1 - P_2$ is usually defined as the greatest pressure reduction which can be sustained

TABLE I. COMPARING THE 14-D, 100-FSW TEKTITE DECOMPRESSION SCHEDULE WITH THE EQUIVALENT 126-FSW VPM SCHEDULE.

Depth (fsw)	Time at stop (min) TEKTITE	Time at stop (min) VPM
100-90	10 normoxic	
90	60 normoxic	
85	90 normoxic	36 air
80	100 normoxic	159 air
75	110 normoxic	165 air
70	120 normoxic	170 air
65	360 normoxic	176 air
60	140 normoxic	182 air
55	160 normoxic	190 air
50	160 normoxic	197 air
45	10 oxygen 150 normoxic	205 air
40	130 normoxic	214 air
35	20 oxygen 150 normoxic	224 air
30	360 normoxic	235 air
25	30 oxygen 150 normoxic	246 air
20	150 normoxic	260 air
15	50 oxygen 150 normoxic	273 air
10	160 normoxic	290 air
5	60 oxygen	308 air
Total:	2960 normoxic + 170 oxygen	3530 air

without the onset of decompression sickness. This condition can be simulated by selecting dives with bottom times of 720 min and by taking P_2 to be the depth of the first decompression stop. The simulation provides a reasonable approximation to a single-step decompression in the nucleation-dominated regime because, in this limit, the rate at which gas is permitted to come out of solution is just slightly higher than that which the body can dissipate and therefore tolerate indefinitely.

In the permeable region of the nucleation model ($P_1 < P^* = 9.2$ ATA), this procedure yields a linear relationship,

$$P_1 = 1.372 P_2 + 0.335 \text{ ATA} \quad \text{Eq. 5}$$

which has a correlation coefficient of better than 0.999 for the eight combinations of P_1 and P_2 which were used. Similar expressions,

$$P_1 = 1.375 P_2 + 0.52 \text{ ATA} \quad \text{Eq. 6}$$

and

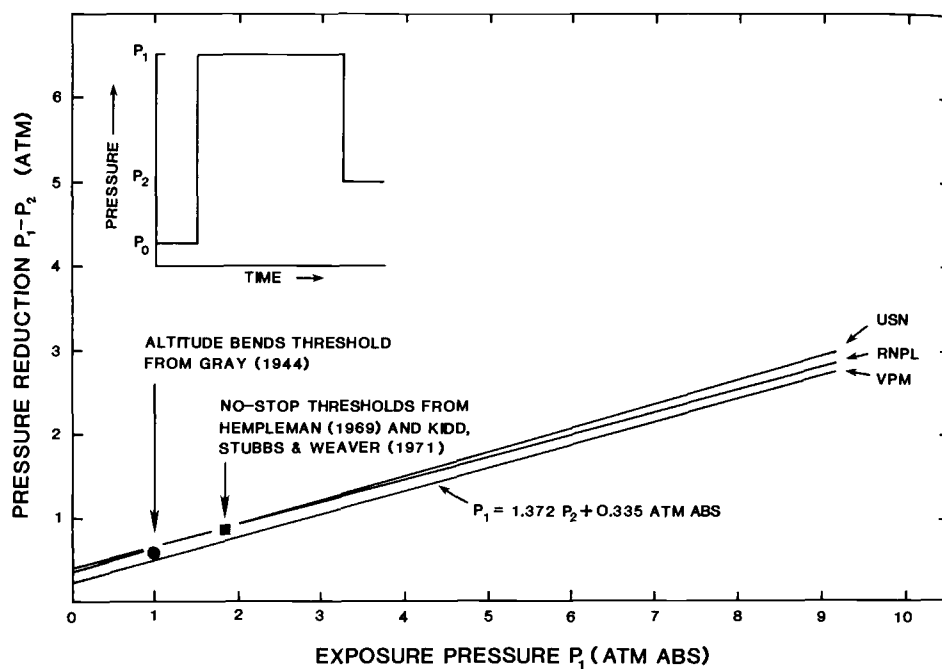


Fig. 5. Allowed pressure reduction $P_1 - P_2$ versus exposure pressure P_1 for USN, RNPL, and VPM air diving tables. In the limit of a nucleation-dominated regime, lines of constant critical volume are also isopleths of constant bubble number.

$$P_1 = 1.366 P_2 + 0.56 \text{ ATA} \quad \text{Eq. 7}$$

have been extracted by Hennessy and Hempleman (7) from, respectively, the USN and RNPL tables.

As can be seen in Fig. 5, the three straight lines are nearly parallel, and VPM is 0.1 to 0.2 atm lower than USN and RNPL. The fact that these lines are similar to the isopleths of constant bubble number presented for the permeable region in Yount (15,16) verifies the above-mentioned correspondence for this rudimentary case. The "no-stop threshold," $P_1 = 1.87 \text{ ATA}$ and $P_1 - P_2 = 0.87 \text{ atm}$, was obtained by averaging the values of $P_1 = 1.90 \text{ ATA}$, $P_1 - P_2 = 0.90 \text{ atm}$ measured by Hempleman (6) with those of $P_1 = 1.83 \text{ ATA}$, $P_1 - P_2 = 0.83 \text{ atm}$ measured by Kidd, Stubbs, and Weaver (8). The VPM result, $P_1 = 1.71 \text{ ATA}$, $P_1 - P_2 = 0.71 \text{ atm}$, is 0.16 atm lower than the experimental average and is therefore "safe." The "altitude bends threshold" plotted in Fig. 5, $P_1 = 1.00 \text{ ATA}$, $P_1 - P_2 = 1.00 - 0.40 = 0.60 \text{ atm}$, was calculated from the value of $P_2 = 7550 \text{ m} = 307 \text{ mm Hg} = 0.40 \text{ ATA}$ measured by Gray (5). The VPM limit of $P_1 = 1.00 \text{ ATA}$, $P_1 - P_2 = 0.52 \text{ atm}$ is again slightly lower, this time by 0.08 atm.

In contrast, the lines for USN and RNPL are both slightly higher than the experimental no-stop and altitude-bends thresholds plotted in Fig. 5. This illustrates the type of problem one encounters in attempting to extrapolate conventional tables that are based upon trial-and-error rather than a global theory. Because of such problems, altitude bends and decompression sickness are usually investigated separately, as if they were different subjects.

DISCUSSION

The immediate goal of this study was not to produce an operational set of diving tables but instead to determine whether a reasonable and comprehensive set

of such tables could be computed from a bubble nucleation model using a modest number of assumptions, equations, and parameter values. The answer to this question, quite obviously, is yes.

The definition of "reasonable and comprehensive" used in this work was "similar, both in scope and in total decompression time, to other tables now in use." A possible criticism of this approach is that some of the reference tables are not very safe, and it may have been a mistake to try to match them, for example, by abandoning the original goal of zero or constant (but physiologically insignificant) bubble number. Alternatively, the opportunity to shorten decompression obligations and improve diving efficiency may have been lost. This is a matter of judgement in which a decision was made to accept the whole range of diving experience, including conventional tables, as useful experimental data. Greater safety and/or efficiency may then become feasible later, both through the unification and "smoothing" which result when a global theory is applied to a broad data base.

Very little has been said about the physiological processes which presumably underlie the mathematical equations. Oxygen and carbon-dioxide were taken into account (22), and a typical range of tissue half-times was assumed (1,14). However, no distinction was made between "fatty, loose tissue" and "watery, tight tissue" (7), nor was it stated explicitly where the bubbles form or how they grow, multiply, or are transported. Finally, nothing was said about such factors as solubility, diffusion versus perfusion, tissue deformation pressure, or tissue-specific differences in surface tension. Since all of the omitted items are poorly understood, at least *in vivo*, the main effect of taking any of them into account is to increase the number of adjustable parameters. In the present case, for example, this number could be doubled simply by assuming a

different set of nucleation parameters for aqueous and lipid constituents. It is therefore a remarkable feature of the nucleation approach—evident already in this naive formulation—that the usual proliferation of free parameters can be avoided.

One by-product of this investigation is an improved understanding of practical decompression tables now in use. It is evident, for example, that profuse bubble formation is permitted by such tables, particularly during dives of short duration. Meanwhile, the number of primary bubbles, i.e., bubbles that form directly from nuclei rather than from other bubbles, is allowed to vary widely. The common assumption that the volume of released gas is critical seems still to be viable providing allowance is made for the body's ability to dissipate free gas at a useful rate.

ACKNOWLEDGMENTS

Four visitors from the École Centrale des Arts et Manufactures, Chatenay-Malabry, France have participated in this program: Gilbert Grenié in 1980, Bernard Rémy in 1981, Gildas Herjean in 1982, and Philippe Mazas in 1983. It is a pleasure also to thank our colleagues Ed Beckman, Claude Harvey, Jon Pegg, and Birch Porter for useful suggestions and comments. This work, carried out under "The Physics of Gas Bubbles: Medical Applications" Project (HP/R-4), is a result of research sponsored in part by the University of Hawaii Sea Grant College Program under Institutional Grant Number NA81AA-D-00070 from NOAA Office of Sea Grant, U.S. Department of Commerce. This is Sea Grant Publication Number UNIHI-SEAGRANT-JC-85-14.

APPENDIX

P_{ss}^{min} in Eq. 3 can be viewed as a safe-ascent criterion based on critical bubble number (15,16). This has been superseded in the present work by a critical-volume hypothesis via P_{ss}^{new} in Eqs. 4a-c. Whereas Eq. 3 follows directly from the varying-permeability model (18), the derivation of Eqs. 4a-c. is heuristic and involves a number of *ad hoc* assumptions, some of which have been discussed already in the methods section. The first, of course, is that the total volume of free gas in the body at any time t should never exceed some critical value V_{crit} . Similarly, the rate at which the gas phase inflates is assumed to be proportional to $P_{ss}^{new}(t)(N_{actual} - N_{safe})$. The decompression criterion is then

$$\int_0^t P_{ss}^{new}(t)(N_{actual} - N_{safe})dt \leq \alpha V_{crit} \quad \text{Eq. A-1}$$

where α is a proportionality constant. To minimize the total decompression time t_D , the equals sign is adopted.

Next it is assumed that N_{actual} and N_{safe} are determined by the initial decompression step and remain constant thereafter. The decompression criterion can then be expressed as

$$\alpha V_{crit} = (N_{actual} - N_{safe}) \int_0^{t_{max}} P_{ss}^{new}(t) dt, \quad \text{Eq. A-2}$$

where t_{max} is that time at which the integral reaches its maximum.

To evaluate the integral, it is assumed that $P_{ss}^{new}(t)$ is held at a constant level P_{ss}^{new} during t_D and decays exponentially to zero thereafter. The fact that $P_{ss}^{new}(t)$ is always positive and never exceeds its initial value P_{ss}^{new} is consistent with the previous assumptions that N_{actual} and N_{safe} are constant. The exponential decay to zero is a conservative approximation since humans equilibrated at atmospheric pressure are "inherently unsaturated" by some 54 mm Hg (22), and $P_{ss}^{new}(t)$ would eventually become negative by this modest amount.

Because $P_{ss}^{new}(t)$ decays exponentially to zero and does not become negative in this formulation, the integral achieves its maximum value in the limit as t_{max} approaches infinity. This gives:

$$\alpha V_{crit} = (N_{actual} - N_{safe}) \left\{ \int_0^{t_D} P_{ss}^{new} dt + \int_{t_D}^{\infty} P_{ss}^{new} \exp[-(t - t_D)/H^*] dt \right\}, \quad \text{Eq. A-3}$$

$$= (N_{actual} - N_{safe}) P_{ss}^{new} (t_D + H^*), \quad \text{Eq. A-4}$$

where $H^* = H/\ln(2) = H/0.693$ is the exponential decay constant and H is the half-time of the particular tissue compartment being considered.

Since the size distribution of gas nuclei in humans is unknown, it is reasonable to try a decaying exponential of the general form observed *in vitro* (18,23-25):

$$N_{actual} = N_0 \exp(-\beta_0 S r_0^{new} / 2kT), \quad \text{Eq. A-5}$$

$$N_{safe} = N_0 \exp(-\beta_0 S r_0^{min} / 2kT), \quad \text{Eq. A-5}$$

where β_0 is a VPM constant, N_0 is a normalization constant, S is the constant area occupied by one surfactant molecule *in situ*, k is the Boltzmann constant, and T is the absolute body temperature—also assumed to be constant. The decompression criterion can now be written:

$$P_{ss}^{new} = \alpha V_{crit} / [(N_{actual} - N_{safe})(t_D + H^*)], \quad \text{Eq. A-7}$$

where:

$$N_{actual} - N_{safe} = N_0 [\exp(-\beta_0 S r_0^{new} / 2kT) - \exp(-\beta_0 S r_0^{min} / 2kT)]. \quad \text{Eq. A-8}$$

At this point it is assumed that the exponential arguments are small and can thus be expanded to give:

$$N_{actual} - N_{safe} \approx N_0 (\beta_0 S r_0^{new} / 2kT) (1 - r_0^{new} / r_0^{min}). \quad \text{Eq. A-9}$$

This last approximation is in some question since the values of the model parameters are neither fixed nor well-known. If in fact the approximation is not valid, the bubble numbers would correspond to a linear nuclear distribution rather than the linear (small exponent) region of an exponential distribution. At this point the true distribution is unknown.

The radii r_0^{new} and r_0^{min} can be replaced using the VPM equations (18):

$$r_0^{min} = 2(\gamma C - \gamma) / \beta_0, \quad \text{Eq. A-11}$$

$$= 2\gamma(\gamma C - \gamma) / \{\gamma C [P_{ss}^{min} - (P_1 - P_0)(\gamma / \gamma C)]\}, \quad \text{Eq. A-12}$$

$$r_0^{new} = 2\gamma(\gamma C - \gamma) / \{\gamma C [P_{ss}^{new} - (P_1 - P_0)(\gamma / \gamma C)]\}. \quad \text{Eq. A-13}$$

Although these equations apply strictly only to the permeable region of the model, their solutions vary little (less than 3%) compared to the impermeable region solutions for values of P_{crush} below 300 fsw.

Substitution of Eqs. A-12 and A-13 into Eq. A-7 gives:

$$\alpha V_{crit} \approx N_0 \{(\gamma C - \gamma) S / kT\} \frac{(P_{ss}^{new} - P_{ss}^{min}) P_{ss}^{new} (t_D + H^*)}{P_{ss}^{new} - (P_1 - P_0)(\gamma / \gamma C)}. \quad \text{Eq. A-14}$$

Eqs. 4a-c can now be obtained by solving for P_{ss}^{new} . The constant λ can be expressed as:

$$\lambda = \{\gamma C k T / \gamma N_0 (\gamma C - \gamma) S\} \alpha V_{crit}. \quad \text{Eq. A-15}$$

Quantities such as α , S , V_{crit} , N_0 , N_{safe} , and N_{actual} are, of course, absorbed into λ , and their values are never explicitly determined. It can be deduced, however, that for $r_0^{min} = 0.800 \mu\text{m}$, r_0^{new} is in the range $0.205 \leq r_0^{new} \leq 0.797 \mu\text{m}$.

REFERENCES

1. Beckman EL, Smith EM. Tektite II: Medical supervision of the scientists in the sea. *Tex. Rep. Biol. Med.* 1972; 30:155-69.
2. Butler BD, Hills BA. The lung as a filter for microbubbles. *J. Appl. Physiol.* 1979; 47:537-43.
3. D'Arrigo JS. Improved method for studying the surface chemistry of bubble formation. *Aviat. Space Environ. Med.* 1978; 49:358-61.
4. Davson H. A textbook of general physiology. 3rd ed. London: Churchill, 1964:185.

BUBBLE MODEL DIVING TABLES—YOUNT & HOFFMAN

5. Gray JS. Aeroembolism induced by exercise in cadets at 23,000 feet. Committee on aviation medicine report 260. Washington: United States National Research Council, 1944.
6. Hempleman HV. British decompression theory and practice. In: Bennet PB, Elliot DH, eds. The physiology and medicine of diving and compressed air work. Baltimore: Williams & Wilkins, 1969:331-47.
7. Hennessy TR, Hempleman HV. An examination of the critical released gas volume concept in decompression sickness. Proc. R. Soc. Lond. B. 1977; 197:299-313.
8. Kidd DJ, Stubbs RA, Weaver RW. Comparative approaches to prophylactic decompression. In: Lambertsen CJ, ed. Underwater physiology IV: Proceedings of the fourth symposium on underwater physiology. New York: Academic Press, 1971:167-77.
9. Leitch DR, Barnard EEP. Observations on no-stop and repetitive air and oxynitrogen diving. Undersea Biomed. Res. 1982; 9:113-29.
10. Paganelli CV, Strauss RH, Yount DE. Bubble formation within decompressed hen's eggs. Aviat. Space Environ. Med. 1977; 48:48-9.
11. Air diving tables. Alverstoke, Hants; Royal Naval Physiological Laboratory, 1968. (London, HMSO, 1968).
12. Strauss RH. Bubble formation in gelatin: implications for prevention of decompression sickness. Undersea Biomed. Res. 1974; 1:169-74.
13. Strauss RH, Kunkle TD. Isobaric bubble growth: a consequence of altering atmospheric gas. Science 1974; 186:443-4.
14. U.S. Navy Department. U.S. Navy Diving Manual. Washington, DC: U.S. Government Printing Office, 1970; NAVSHIPS 0994-001-9010.
15. Yount DE. Application of a bubble formation model to decompression sickness in fingerling salmon. Undersea Biomed. Res. 1981; 8:199-208.
16. Yount DE. Application of a bubble formation model to decompression sickness in rats and humans. Aviat. Space Environ. Med. 1979; 50:44-50.
17. Yount DE. On the evolution, generation, and regeneration of gas cavitation nuclei. J. Acoust. Soc. Am. 1982; 71:1473-81.
18. Yount DE. Skins of varying permeability: a stabilization mechanism for gas cavitation nuclei. J. Acoust. Soc. Am. 1979; 65:1429-39.
19. Yount DE, Gillary EW, Hoffman DC. A microscopic investigation of bubble formation nuclei. J. Acoust. Soc. Am. 1984; 76:1511-21.
20. Yount DE, Hoffman DC. On the use of a cavitation model to calculate diving tables. In: Hoyt JW, ed. Cavitation and multiphase flow forum-1983. New York: American Society of Mechanical Engineers, 1983:65-8.
21. Yount DE, Hoffman DC. Decompression theory: a dynamic critical-volume hypothesis. In: Bachrach AJ, Matzen MM, eds. Underwater physiology VIII: proceedings of the eighth symposium on underwater physiology. Bethesda: Undersea Medical Society, 1984:131-46.
22. Yount DE, Lally DA. On the use of oxygen to facilitate decompression. Aviat. Space Environ. Med. 1980; 51:544-50.
23. Yount DE, Strauss RH. Bubble formation in gelatin: a model for decompression sickness. J. Appl. Phys. 1976; 47:5081-8.
24. Yount DE, Yeung CM. Bubble formation in supersaturated gelatin: a further investigation of gas cavitation nuclei. J. Acoust. Soc. Am. 1981; 69:702-8.
25. Yount DE, Yeung CM, Ingle FW. Determination of the radii of gas cavitation nuclei by filtering gelatin. J. Acoust. Soc. Am. 1979; 65:1440-50.